Diyala Journal of Engineering Sciences

Journal homepage: https://djes.info/index.php/djes

ISSN: 1999-8716 (Print); 2616-6909 (Online)

A Comparative Investigation on Powder Mixed EDM Machining of Steel Alloys with Multi-Objective Optimization Using Fuzzy-TOPSIS Method

Md Nadeem Alam[1*], Mohd Atif Wahid[2], Raghib Ahsan[3], Naveen Kumar[3] and Shoaib Sabri[4]

[1]Department of Mechanical Engineering, Faculty of Engineering and Technology, Jamia Millia Islamia, New Delhi (110025), India
[2]School of Engineering & Technology, Vivekananda Institute of Professional Studies – Technical Campus, Delhi (110034), India.
[3]School of Engineering and Technology, SHARDA UNIVERSITY, Greater Noida, Uttar Pradesh (201306), India.
[4]Department of Mechanical Engineering, VCTM, AKTU Lucknow, Uttar Pradesh (226031), India.

ARTICLE INFO

Article history:
Received September 4, 2024
Revised October 25, 2024
Accepted November 1, 2024
Available online December 1, 2024

Keywords:
PMEDM process
Surface roughness
MRR
TWR
Fuzzy TOPSIS method
Surface cracks
White layer

ABSTRACT

The current work offers a comparative study that examined the effects of various process parameters, such as dielectric fluid, current (IP), pulse on time (TON), and different conductive powder particles mixed dielectric fluids, on electrical discharge machining (EDM) of AISI 1040, EN31, and HCHCr steels, respectively. The findings indicate that adding conductive particles to the dielectric medium during the powder-mixed EDM (PMEDM) process enhances energy distribution across the spark gap, thereby improving material removal capacity and the surface characteristics of the machined surfaces. Experimental results show that the concentration of powder particles has the most significant impact on surface roughness (Ra) and tool wear rate (TWR), while the most critical factor affecting the material removal rate (MRR) is the current (IP). Additionally, increasing the IP and TON leads to the formation of continuous, thick cracks and a thin white coating on the EDMed surface, as evidenced by scanning electron microscopy (SEM) images of the surface morphology. The study also employs a multi-optimization technique using the Fuzzy-based TOPSIS method to investigate the cumulative effects of the control parameters on performance indicators, namely Ra, MRR, and TWR. In experimental run 8 i.e. moderate IP (5 A), higher TON (180 µs), and higher concentration of copper powder (10 g/l) mixed in EDM oil while machining of AISI 1040, the optimal results i.e. Ra is 5.983 µm, MRR is 27.243 mm^3/min, and TWR is 0.775 mm^3/min were obtained, respectively.

1. Introduction

Steel alloys are increasingly in demand across various industries, including die-making, press tools, cold-forming molds, and automotive sectors, due to their outstanding wear resistance, exceptional dimensional stability, high compressive strength, and superior hardness. These steel alloys are essential in industries such as die-making and automotive i.e. used in manufacturing gears, axles, and other components due to their excellent mechanical properties [1]. These steel alloys pose significant machining challenges due to their work-hardened characteristics, which can result in severe tool wear, compromised surface integrity, and increased manufacturing costs. Traditional machining methods frequently generate high cutting temperatures and surface defects, highlighting the need for alternative approaches [2-4]. Industries require stringent standards for efficient and cost-effective machining techniques when working with these difficult-to-machine materials, ensuring that surface quality and productivity are not compromised. This need drives the search for

* Corresponding author.
E-mail address: mdnadeemalam7@gmail.com
DOI: 10.24237/djes.2024.17402

effective and economical machining solutions for high-strength materials i.e. Non-traditional machining techniques (NTMT).

Non-traditional machining techniques (NTMT) address the limitations of conventional machining methods when working with high-strength materials. Extensive research has been conducted to explore the machining of difficult materials using various NTMT. However, some NTMT face challenges that hinder their industrial application. For instance, abrasive water jet machining (AWJM) is often unsuitable for thick materials and can lead to surface degradation and dimensional inaccuracies [5]. Economically cutting hard materials with ultrasonic machining is also challenging, as high tool wear limits its effectiveness [6]. Additionally, electrochemical machining struggles to produce flat surfaces or sharp corners due to the erosion of sharp profiles [7]. In laser beam machining, thermal energy can create significant recast layers and heat-affected zones (HAZ) due to tapering during the process [8]. Therefore, selecting the appropriate machining process is crucial for producing high-quality components while keeping costs manageable. Even for hard and brittle materials, the electrical discharge machining (EDM) technology has proven to be effective at generating complex profiles with reduced HAZ and dimensional inaccuracies. The machining of hardened steels using EDM improves material removal rate and decreases tool wear rate while preserving higher surface polish [9]. EDM method is a novel thermo-electric approach that widely utilised non-conventional material removal method. Where, the cold emission of electrons from the cathode ionizes a thin film, creating a highly conductive ionized column (spark) that is used for machining operations. The spark gap is the opening that allows the maximum electric field to be maintained at the smallest possible distance between the tool and the workpiece. The spark gap is maintained by a servo control unit, which is identified by the average voltage across the gap. A suitable voltage is created across the electrodes as a result of this minimum gap, which creates an electrostatic field strong enough to cause cold emission of electrons and produce an electric spark. The workpiece's temperature instantly rises to 10,000 0C due to the spark across the spark gap [10, 11]. In general, it is used for the die industries, automobile industries, and aerospace industries. It can be used to successfully process conductive materials with a range of toughness and hardness. Despite the process' incredible merits, EDM has a number of limitations, including poor surface quality and low material removal rate [11].

In this situation, the powder mixed EDM (PMEDM) technology has emerged as a revolutionary method for boosting the process abilities. It involves mixing of appropriate powder particles into the dielectric fluid (D_F), causing a skinny layer of additive particles of powder mixed D_F through the spark gap (S_G) that develop the capabilities of the EDM process, where the particles of conductive powder lessen the insulating resilience of the D_F and elevate the S_G through the electrodes, which allows the process to be more reliable and enhancing the surface eminence and material removal of the component [11, 12].

The PMEDM method is illustrated in Figure 1, where the powder particles are blended with the D_F either in the same vessel or in separate container. According to Kansal et al. (2007), adding conductive powder to the mixed dielectric fluid across the spark gap can significantly increase the gap distance, sometimes doubling or even more. In this process, the electrified powder particles flow in a criss-cross pattern, causing the grains to move closer together in the spark region and aggregate into clusters. Furthermore, electric forces allow the powder particles to create small chains in several segments across the igniting region that assists in bridging the S_G [10]. Bridging weakens the insulating strength of D_F and lowers the gap voltage, culminating in an easy short-circuit and quick explosion throughout the S_G, causing a series of electric discharges throughout the machining area. These electric discharge triggers the erosion and vaporisation of the material [12].

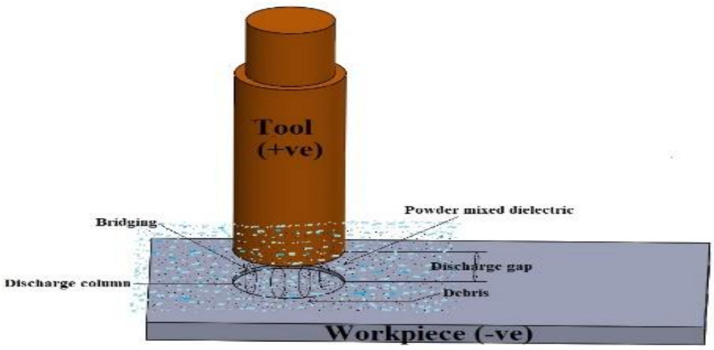

Figure 1. Principle of PMEDM process

If the spark dispersion among the powder particles is uniform, a series of narrow craters typically forms on the EDM-ed surface, resulting in an improved surface finish [11]. Additionally, the mixing of conductive powder particles increases the frequency of discharges, which enhances spark intensity and promotes greater workpiece erosion. This accelerated erosion contributes to higher material removal rates (MRR) and increased surface roughness (Ra). Conductive powders also help dissipate the heat generated during the EDM process, minimizing thermal damage to both the workpiece and the wire. Furthermore, the addition of powder enhances the plasma channel, further improving machining performance [12-13].

Numerous studies have examined the impact of various control parameters on the capabilities of the powder-mixed EDM (PMEDM) process. Research has shown that the PMEDM technique is effective in enhancing surface characteristics and machining performance [11, 13]. According to Bains et al. (2019), the magnetic field significantly influences the material removal rate (MRR) and surface roughness (Ra) in traditional EDM processes, while also reducing the thickness of the recast layer (t_R). They observed that combining a magnetic field with low current (I_P) and extended pulse-off time (T_{OFF}) minimized particle re-sticking on the machined surface and significantly improved flushing capacity. As a result, they recorded a 118% increase in MRR, a 67.5% reduction in Ra, and a 63% increase in machining efficiency (MH) [14]. Hameed et al. (2019) compared the performance of several powders (manganese (Mn), aluminium (Al), and a mixture of Mn-Al mixed DF) during EDM of various steel alloys, such as D3 steel, H13 steel, and D6 steel. The results showed that, in comparison to other dielectric mixtures, Mn powder combined DF gives the highest surface micro hardness [15]. In the investigation of the impact of silicon (Si) and copper (Cr) powder mixed kerosene D_F on the TWR of the Cu tool during EDM of AISI D2 steel, Kazi et al. (2020) came to the conclusion that Cr mixed D_F results in lower TWR when compared to Si powder mixed D_F [16]. According to Singh and Singh (2022), the ultrasonic-assisted EDM (UAEDM) technique has greater MRR and Ra values than the conventional EDM process. This is because the UAEDM process, which involves the tool electrode moving back and forth, causes a considerable pressure change within the inter-electrode gap (IEG), allowing debris particles to be ejected from the IEG and improving flushing. Additionally, they came to the conclusion that when compared to the traditional EDM method, the UAEDM process leads in a 53.57 percent improvement in MRR and an 18.47 percent increase in Ra [17]. Zhang et al. [18] explored a transverse magnetic field-assisted wire electrical discharge machining (WEDM) process to improve the uniformity of discharge point distribution and reduce alterations during the machining of thin-wall components in WEDM-low speed (WEDM-LS). They found that the longitudinal dispersion uniformity of discharge points increased with higher magnetic field strength, achieving the highest improvement of 12.32% at a magnetic field strength of 0.15 T. Additionally, the application of the transverse magnetic field led to a 32.77% reduction in distortion and a 22.68% decrease in the recast layer thickness.

In addition to selecting the appropriate process parameters, choosing an effective optimization technique is essential for maximizing performance characteristics. Several studies have focused on identifying the best optimization strategies. Multi-criteria decision-making (MCDM) approaches are necessary for selecting optimal control parameters to achieve improved performance characteristics in the PMEDM process, especially when dealing with conflicting features.A fuzzy-based grey relation analysis (GRA) algorithm has successfully identified the optimal material removal rate (MRR) and tool wear rate (TWR). The results indicated that all control parameters and their combinations significantly affect the MRR, except for the combination of current (IP) and gap voltage (VG). In contrast, for TWR, all control parameters and their combinations significantly influence the rate, except for pulse-on time (TON) and the combination of IP and TON [19].Sivapirakasam *et al.* (2011) established a Taguchi-based fuzzy TOPSIS approach to address multiple response optimization problems in the green EDM process, where triangular fuzzy numbers were used to acquire the weights for different output responses, and the utmost predicted factor level arrangements were assigned using the TOPSIS method. This method's basic philosophy is to choose the finest alternative with the lowest and greatest distance from the positive and negative ideal solutions, respectively [4]. Real-world multi-criteria decision-making (MCDM) problems often involve ambiguous, imprecise, and interpretive data, which complicates the decision-making process. In evaluating such data, decision-makers typically account for risk using linguistic variables like low, high, very high, and very low. Fuzzy set theory effectively addresses this ambiguity, allowing for the use of linguistic variables for generalization [20]. Among the available methods, the TOPSIS (Technique for Order of Preference by Similarity to Ideal Solution) approach stands out as a robust solution for tackling multiple response optimization problems that involve both discrete and continuous data across various industrial applications. However, the TOPSIS method is the best solution for dealing with multiple response optimization issues that have both discrete and continuous data in various industrial applications. Further, it was witnessed that the best-chosen option is the one that is nearby the positive ideal solution (V^+) and the utmost away from the negative ideal solution (V^-) [21].

The investigation on several MCDM approaches revealed that the TOPSIS method is the most effective method for solving complicated response optimization problems, particularly in commercial applications that involve both discrete and continuous data. It is clear from the reported literature that very less research has been done to examine the combined effects of various tool materials, varied powder combinations, and variable concentration dielectric fluids during EDM of various steel grades. Therefore, the current study focused on the PMEDM of different steel alloys viz. American Iron and Steel Institute (AISI) 1040, European standard (EN) 31, and High Carbon High Chromium (HCHCr) steel, using various electrode materials (M_E), various powder materials (M_P), with adding different concentration of powder particles in EDM oil and kerosene, respectively. The effect of different process parameters viz. current and pulse on time on PMEDM performance characteristics was also investigated. Further, a fuzzy based TOPSIS method was employed to found optimum set of input parameters which avails the optimal result of multiple responses i.e. Ra, MRR, and TWR. The study directly addresses industry challenges by focusing on real-world applications and optimizing processes for high-strength materials, which is crucial for improving manufacturing efficiency. PMEDM is an advanced machining process where fine powder particles mixed dielectric fluid used to enhances the machining process by improving surface quality of the product which enhances the service life of the product, increasing MRR which leads to improve productivity, and reducing TWR which may cause for enhancing tool life. All these scenario leads to optimizing the overall manufacturing cost of the product.

2. Experimental setup and methodology

2.1. Experimental setup

The set of 18 experiments were performed in the MITSUBISHI ELECTRIC (Japan) made D-7120 die-sink EDM machine in the presence of EDM oil and kerosene as dielectric media mixed with different powder particles of average size 100 micron procured from SAVEER MATRIXNANO PRIVATE LIMITED. Figure 2 shows the illustration of PMEDM process.

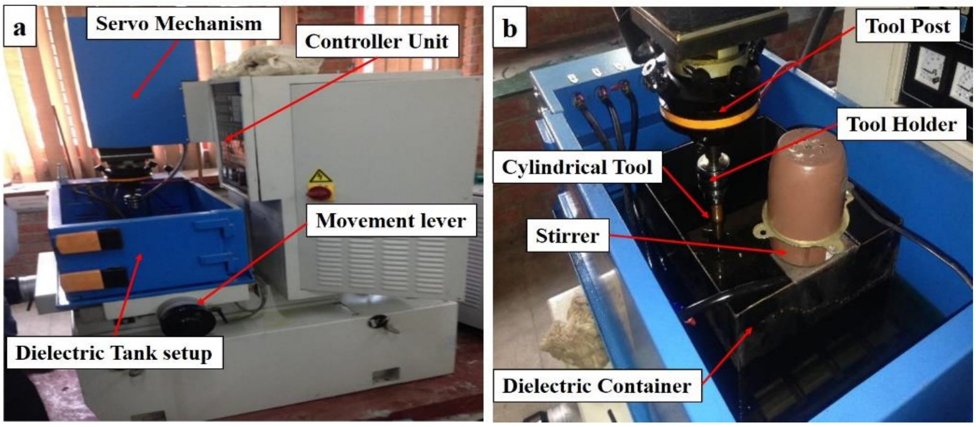

Figure 2. Illustration of D-7120 Die-sink EDM machine

Various suitable conductive powder mixed DF was used in the present work, where a stirrer setup was attached (Figure 2b) to improve mixing and circulation of the powder particles into the dielectric media. Figure 3 depicts the EDMed specimens of EN 31, AISI 1040, and HCHCr. Each of the workpiece sample had the following measurements: 60 × 30 × 10 mm (refer Figure 3). Table 1 displays the chemical configuration of the various elements in the chosen steel alloys.

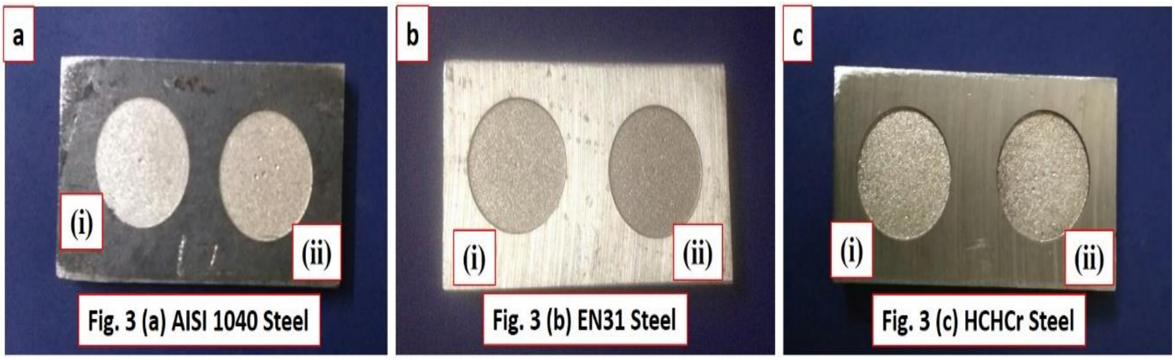

Figure 3. EDMed samples of (a) AISI 1040, (b) EN31, and (c) HCHCr steel alloys

Table 1: Chemical arrangement of following steel alloys

Workpiece	% arrangement								
	C	Mn	S	P	Cr	Si	Ni	Cu	Mo
AISI 1040	0.400	----	0.050	0.040	----	----	----	----	----
EN-31	1.100	0.600	0.500	----	1.400	0.250	----	----	----
HCHCr	1.500	0.060	0.030	0.030	12.000	0.600	0.300	0.250	0.900

EDM of the foregoing materials is carried out using three distinct tool materials, where, all the tools were shaped as cylindrical bar of diameter 20 mm. The diameter of cylindrical tools was measured using digital Vernier calliper (Mitutoyo Japan). Table 2 depicts the chemical arrangement of the selected tools. However, the physical properties of selected powders and D_F are noted in Table 3 and Table 4, respectively.

Table 2: Chemical arrangement of selected tool materials

Tool	% arrangement							
	W	**Cu**	**Ni**	**Z**	**Ti**	**Pb**	**C**	**Cr**
Cu	---	99.78	0.045	0.09	0.029	0.044	---	---
W-Cu	79.36	19.462	0.121	0.047	0.014	0.026	---	---
Graphite							100	

Table 3: Physical properties of powder particles

Powder	Density (g/cm^3)	Melting point (^{0}C)	Thermal conductivity (W/mK)	Electrical conductivity (S-m)
Copper	8.96	1085	385	$5.85*10^7$
Chromium	7.18	1857	93.9	$0.77*10^7$
Tungsten	19.6	3244	175	$1.79*10^7$

Table 4: Properties of selected dielectric fluids

Dielectric fluid	Dynamic viscosity (g/ms)	Density (g/mm^3)	Breakdown voltage (kV/mm)	Thermal conductivity (W/mK)	Specific heat (J/gK)	Dielectric constant
EDM oil	0.92-1.0	1000	65-70	0.606-0.62	4.19	80.4
Kerosene	1.64	781	14-22	0.14-0.149	2.1-2.16	1.8

2.2. Methodology

2.2.1. Design of experiments (DOE)

To perform the set of experiments Taguchi's orthogonal array (OA) was used to create design of experiments (DOE) using Minitab-18 software and Microsoft Excel was used for implementing the fuzzy TOPSIS method. Taguchi technique is based on 'orthogonal array', which requires minimum number of experimental data to demonstrate maximum information regarding all the control factors that affects the output responses and design an optimised setting of control parameters to obtain the best result possible for the experiments, also generates mean and (signal to noise ratio) S/N ratio graph which shows the impact of different control parameters on the selected responses. In this analysis, the control parameters and their levels are displayed in Table 5. The levels of the input parameters are obtained from pilot study which helped to identify the range and optimum setting for each factor.

Table 5: Selection of factors and their levels

S.NO.	Control Parameters (units)	Factor Designation	Level-1	Level-2	Level-3
1.	Dielectric fluid	A	EDM Oil	Kerosene	
2.	Workpiece	B	AISI 1040	EN 31	HCHCr
3.	Current (A)	C	3	5	7

4.	Pulse on time (µs)	D	60	120	180
5.	Electrode	E	Copper	Tungsten Copper	Graphite
6.	Types of powder	F	Copper	Chromium	Tungsten
7.	Powder Concentration (gm/l)	G	0	5	10

Table 6 lists the series of 18 tests that are being conducted and includes the mean values for the measured response variables Ra, MRR, and TWR. Using Taguchi L18 orthogonal array allows for the efficient evaluation of multiple factors (up to 18) with a limited number of experiments (18 runs), which optimizes experimental time and cost. The Ra values were determined using the SJ 210 Mitutoyo portable surface roughness tester. When the surface roughness tester's stylus passes over a machined surface, the average surface roughness value is measured.

Table 6: L_{18} experimental design with response variables

S.NO:	D_F	M_W	I_P (A)	T_{on}, (µs)	M_E	M_P	C_P (g/l)	Mean S_R (µm)	Mean MRR (mm^3/min)	Mean TWR (mm^3/min)
1	EDM oil	HCHCr	3	60	Cu	Cu	0	3.553	9.321	0.919
2	EDM oil	HCHCr	5	120	W-Cu	Cr	5	5.633	16.003	0.875
3	EDM oil	HCHCr	7	180	Graphite	W	10	9.348	32.999	1.560
4	EDM oil	EN31	3	60	W-Cu	Cr	10	2.677	8.065	0.630
5	EDM oil	EN31	5	120	Graphite	W	0	9.910	22.992	1.755
6	EDM oil	EN31	7	180	Cu	Cu	5	10.748	26.149	1.196
7	EDM oil	AISI1040	3	120	Cu	W	5	4.137	20.893	0.955
8	EDM oil	AISI1040	5	180	W-Cu	Cu	10	5.983	27.243	0.775
9	EDM oil	AISI1040	7	60	Graphite	Cr	0	11.798	18.253	1.361
10	Kerosene	HCHCr	3	180	Graphite	Cr	5	6.932	17.116	1.178
11	Kerosene	HCHCr	5	60	Cu	W	10	2.278	18.339	0.911
12	Kerosene	HCHCr	7	120	W-Cu	Cu	0	8.847	17.598	1.399
13	Kerosene	EN31	3	120	Graphite	Cu	10	6.488	21.383	0.868
14	Kerosene	EN31	5	180	Cu	Cr	0	12.826	19.270	1.473
15	Kerosene	EN31	7	60	W-Cu	W	5	5.698	21.313	1.151
16	Kerosene	AISI1040	3	180	W-Cu	W	0	7.618	16.899	1.153
17	Kerosene	AISI1040	5	60	Graphite	Cu	5	6.162	20.293	0.836
18	Kerosene	AISI1040	7	120	Cu	Cr	10	8.332	24.996	1.054

2.2.2. Fuzzy TOPSIS method

A fuzzy-based TOPSIS approach, a multi-criterion decision-making (MCDM) method, has been employed to address the multi-response optimization problem in the PMEDM process. This approach is particularly useful for resolving practical issues when individual preferences are expressed through linguistic data. The linguistic information was represented using triangular fuzzy numbers, as illustrated in Table 7. Four experts—two from industry and two from academic institutions—contributed to the decision-making process. As outlined in Table 8, each decision maker (DM) assessed the weight of the response variables using linguistic terms. Table 9 presents the total fuzzy weight assigned to each response variable. Furthermore, the linguistic scores from all sets of response variables (criteria) collected during each experimental operation (alternative) were utilized to construct the fuzzy decision matrix and the normalized fuzzy decision matrix (NFDM).

Additionally, it was considered that the rates of each criterion would lead to the identification of fuzzy positive (V+) and fuzzy negative (V-) ideal solutions. The closeness coefficients for each alternative were calculated, allowing for the determination of the best ranking based on the specified criteria. In this method, the weighted performance matrix is measured by the product of associated weight, NFDM and the fuzzy waiting of alternatives at the response variable w_{ij} ; where i = 1, 2, ….., m, j = 1, 2, ….,n, and m signifies the number of alternatives, and n indicates the number of criteria. The NFDM was determined using equation (1).

$$r_{ij} = \frac{x_{ij}}{\sqrt{\sum_{i=1}^{18} x_{ij}^2}} \quad (1)$$

In equation (1), x_{ij} signifies the authentic value of ‘i'th criteria of jth alternative and r_{ij} signifies the equivalent normalized value. Further, the values of NFDM were multiplied by the associated weights of each criterion to produce the weighted performance matrix (W). Furthermore, the positive ideal value set (W^+) and negative ideal value set (W^-) were computed by using equation (2), and (3) [20].

W^+ = {[max(W_{ij}) j ϵ J_1] or [min(W_{ij}) j ϵ J'], i = 1, 2,….18} (2)

W^- = {[min(W_{ij}) j ϵ J_1] or [max(W_{ij}) j ϵ J'], i = 1, 2,….18} (3)

where J = {j = 1, 2, and 3|j}: denotes the greater the better criteria, J' = {j = 1, 2, and 3|j}: denotes the lower the better criteria. In the existing investigation, MRR is assumed to be the greater the better type, whereas Ra and TWR are assumed to be the lower the better types.

Table 7: Linguistic variables for the significance of fuzzy weighting of each criterion [20]

Linguistic Significance	Abbreviation	Fuzzy Scale
Extremely low	EL	(0, 0, 0.1)
Very low	VL	(0, 0.1, 0.3)
Low	L	(0.1, 0.3, 0.5)
Medium	M	(0.3, 0.5, 0.7)
High	H	(0.5, 0.7, 0.9)
Very High	VH	(0.7, 0.9, 1)
Extremely High	EH	(0.9, 1, 1)

Table 8: Significance of nominated criteria’s (response variables)

Output response	Decision Maker			
	DM1	DM2	DM3	DM4
Surface Roughness (Ra)	VH	VH	H	VH
Material Removal Rate (MRR)	VH	EH	EH	VH
Tool Wear Ratio (TWR)	H	H	H	H

Table 9: Fuzzy weight of nominated criteria’s

Output responses	Fuzzy weight
Surface Roughness (Ra)	0.65, 0.85, 0.975
Material Removal Rate (MRR)	0.8, 0.95, 1
Tool Wear Ratio (TWR)	0.5, 0.7, 0.9

4. Results and discussion

This paper investigates the PMEDM process and the effect of various control parameters on different output responses including Ra, MRR, and TWR.

4.1. Investigation of surface roughness (Ra)

The crater size produced and the dispersion of recast layer on the machined surface are used to estimate the surface quality of the EDMed surface [11, 22]. The experimental results witnessed that the Ra value of distinct steel alloys differs within the range of 2.278 µm to 12.826 µm that can be professed from main effect plot (Figure 4).

Figure 4 shows that as I_P and T_{ON} increase, the Ra value also increases because it has a wide surface area and strong dispersive energy, which results in powerful spark and impulsive forces that grow larger as Ra increases [23]. Furthermore, tungsten (W) powder mixed with the dielectric resulted in the lowest surface roughness (Ra), followed by copper (Cu) powder and chromium (Cr) powder mixed dielectrics. This can be attributed to the combined effects of the high density (ρ) and thermal conductivity (k) of W particles compared to Cu and Cr particles. Higher ρ and k lead to smaller craters on the machined surface, as they influence the plasma generated and promote a uniform distribution of spark energy in the machining zone, thereby reducing Ra [24, 25]. Additionally, increasing the concentration of powder significantly decreases Ra. The accumulation of more powder particles produces shorter pulses even at wider spark gaps. These short pulses distribute the intensity of spark energy across multiple locations within the specified pulse duration, resulting in smaller and narrower craters on the workpiece surface, which contributes to a lower Ra. However, adding excessive powder can complicate the stirring of the fluid mixture, as the particles tend to settle in the tank, negatively affecting the surface properties [25]. Figure 5 displays the S/N ratio plot for the influence of input parameters on Ra value.

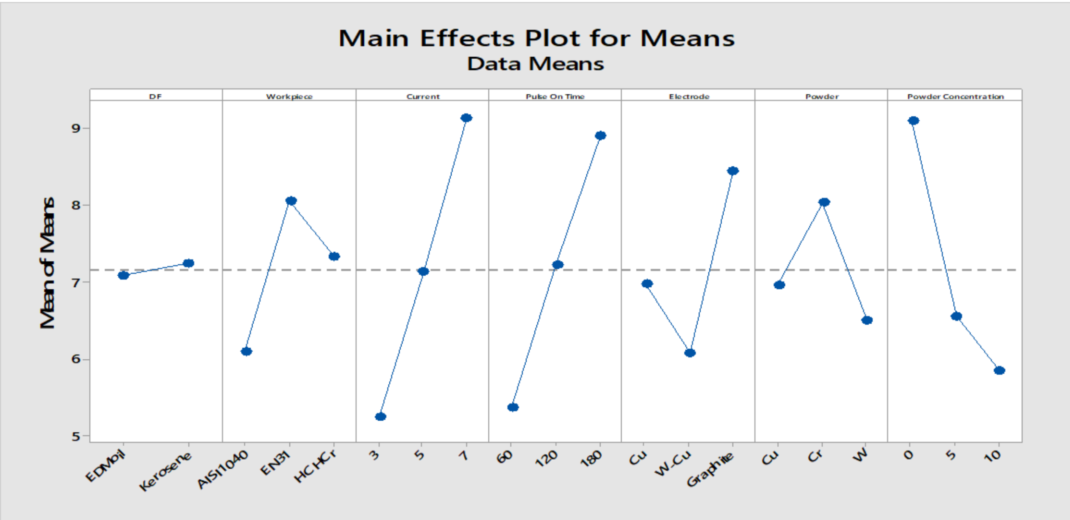

Figure 4. Main effect plot for control parameters (X-axis) on Ra (Y-axis)

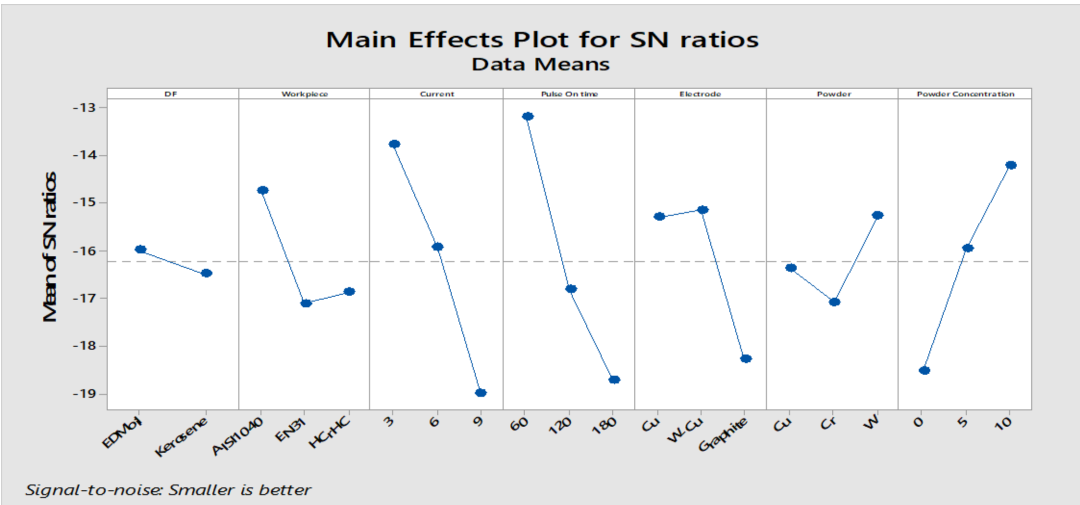

Figure 5. S/N ratio analysis for various control parameters on Ra

Ra is minimally influenced by the type of dielectric fluid (DF), but EDM oil results in a higher Ra compared to kerosene. This is due to the faster-moving molecules in EDM oil, which contribute to increase arcing during the machining process. As shown in Figure 6, the W-Cu tool produces a superior surface finish compared to both the Cu electrode and the graphite tool. This can be attributed to the lower electrical conductivity of the W-Cu alloy. The electrical conductivity of the tool material plays a crucial role in the EDM process, as it affects the characteristics of spark generation. Low conductivity of the tool electrode causes less spark intensity, as a result, narrow craters on the workpiece surface, resulting in low Ra [22]. Additionally; it is shown that PMEDM of an AISI 1040 steel surface is the best quality surface, followed by HCHCr steel and EN 31 steel. This may be attributed as the low carbon and sulphur content present in AISI 1040 steel which leads to the low production of spark energy than EN 31 and HCHCr steel and resulting for low Ra of machined surface [26].

Ra is a significant PMEDM response variable that has been quantified and indicated in Table 6. The impact of various control parameters and their significance on the Ra were assessed using the Analysis of Variance (ANOVA) approach which is an essential analytical method for locating significant components. The ANOVA method's findings show that the I_P, T_{ON}, M_E, and C_P all have a sizable impact on the Ra of different steel alloys. However, it is clear that D_F has the least significant impact on Ra. T_{ON} (31%), I_P (27%), and C_P (19%) are possibly the elements that have the most of an impact on Ra, as seen in Figure 6. Table 6 shows that the minimum Ra value of 2.278 µm is acquired when machining HCHCr steel with W powder mixed kerosene D_F and Cu electrode at 5 An I_P and 60 µs T_{ON}.

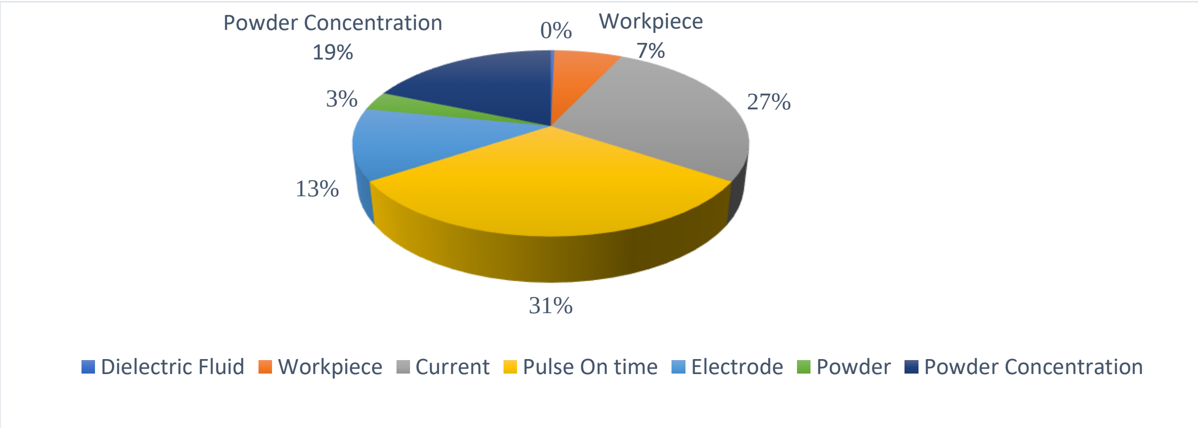

Figure 6. Percentage contribution of alternative control parameters that influence Ra

Table 10: Analysis of variance for mean of Ra

Source	DF	Seq SS	Adj SS	Adj MS	F	P
DF	1	0.108	0.1079	0.1079	0.21	0.674
Workpiece	2	11.785	11.7849	5.8925	11.24	0.023
Current	2	45.501	45.5009	22.7504	36.06	0.003
Pulse On Time	2	37.800	37.7997	18.8999	43.41	0.002
Electrode	2	17.076	17.0758	8.5379	16.29	0.012
Powder	2	7.432	7.4321	3.7161	7.09	0.048
Powder Concentration	2	34.894	34.8938	17.4469	33.29	0.003
Residual Error	4	2.096	2.0965	0.5241		
Total	17	156.692				

According to Taguchi, there are two methods for finishing the analysis. First, the primary method, which uses analysis of variance (ANOVA) to process the average of the repeated runs and the results of a single run. Applying the S/N (signal-to-noise) ratio for the identical steps in full analysis is the other technique that Taguchi strongly recommends for the multiple runs. The concurrent quality matrix, or S/N ratio, is linked to the loss functions. ANOVA is performed to examine the significance of the control parameters. Table 10 shows the ANOVA table for mean of Ra. Table 10 reveals that the control parameters with p-value less than 0.05 significantly affect the multiple output characteristic i.e. Ra value. From Figure 6 and Table 10 it can be seen that T_{ON} is the most significant factor influencing Ra.

4.2 Investigation of material removal rate (MRR)

MRR, which measures material erosive rate during machining and characterises the effectiveness of the operation, by raising MRR. Main objective of machining is to boost productivity and generate value. The value of MRR can be quantified as the weight difference between the workpiece before and after machining as a function of material density (ρ) in g/mm^3 and machining time (t) in minutes which is shown in Eqn. (4) [20].

$$MRR = \frac{Wo - Wf}{\rho * t} \quad (4)$$

Where, Wo = Workpiece weight before machining (g), Wf = Workpiece weight after machining (g)

In general, the chosen material has good conductivity, hardness, and a high melting point. The experimental analysis showed that the MRR value of various steel alloys ranges from 8.065 mm^3/min to 32.999 mm^3/min. The main effect plot Figure 7 shows that increasing I_P and T_{ON} increases the MRR value significantly.

This is supported by the observation that increasing the input pulse (I_P) and pulse-on time (TON) significantly enhances the spark energy during the EDM process, leading to a greater removal of material from both the tool and the workpiece [27]. Additionally, increasing powder accumulation improves the material removal rate (MRR). This improvement occurs because adding conductive particles to the dielectric fluid (D_F) facilitates spark gap (S_G) breakdown and raises the spark gap between electrodes, reducing the DF's insulating strength and making short circuits more likely. This results in rapid sparking and explosive discharge, which accelerates material erosion and increases MRR [28]. The influence of different powder particles on MRR can be attributed to their physical properties, such as thermal conductivity, electrical conductivity, and density. Tungsten and copper, with their relatively high electrical and thermal conductivities, weaken the insulating properties of the D_F and efficiently dissipate heat, enhancing material removal [29]. It is often observed that the graphite tool achieves the highest removal rate for steel alloys, followed by the copper tool and the W-Cu tool. This trend can be traced to the high electrical conductivity of the graphite tool, followed by copper and then W-Cu. The increased electrical conductivity of the tool raises spark intensity, which not only boosts the removal of workpiece material but also affects the removal of tool material.

Furthermore, when compared to kerosene D_F, EDM oil produces a high MRR. In contrast to EDM oil, kerosene's decomposed carbon builds up on the workpiece's surface as a carbide layer. These layers prevent further erosion of both electrodes, but in the case of EDM oil, a layer of oxide is formed over the surface of the workpiece that is easily breakable even at lower temperatures, increasing the MRR [30]. Furthermore, EDM of HCHCr steel allows easy material removal, followed by EN 31 and AISI 1040 steel. This could be due to the high carbon percentage in HCHCr steel, which was followed by EN 31 and AISI 1040 steel. Figure 8 displays the S/N ratio plot for the influence of input parameters on MRR value.

The ANOVA method can be used to determine the effect of different control parameters on the MRR, and their relative relevance was indeed estimated. The three most significant variables affecting MRR are the I_P, T_{ON}, and M_P, as shown in Figure 9. The least significant element affecting MRR is discovered to be the kind of D_F. The most significant variables affecting MRR, as shown in Fig. 9, are I_P (35%), T_{ON} (29%), and M_P (12%), respectively. Table 6 signifies that the maximum MRR value of 32.999 mm^3/min is achieved while machining HCHCr steel using a mixture of EDM oil and tungsten powder with a graphite tool at 7 An I_P and 180 µs T_{ON}.

Further, ANOVA is performed to examine the significance of the control parameters on MRR. Table 11 shows the ANOVA table for mean of MRR. Table 11 reveals that the control parameters with p-value less than 0.05 significantly affect the multiple output characteristic i.e. MRR value. From Figure 9 and Table 11 it can be seen that I_P is the most significant factor influencing MRR.

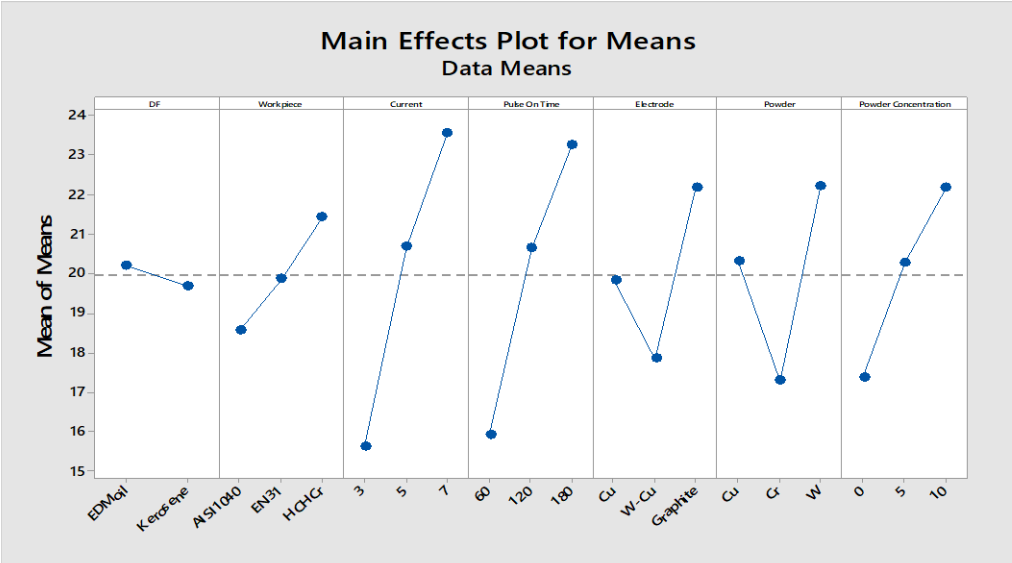

Figure 7. Main effect plot for control parameters (X-axis) on MRR (Y-axis)

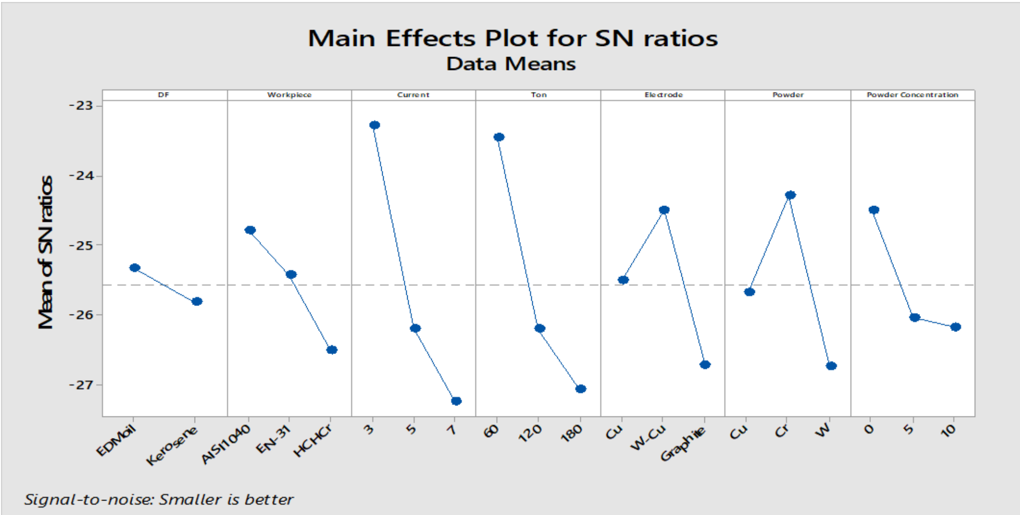

Figure 8. S/N ratio analysis for various control parameters on MRR

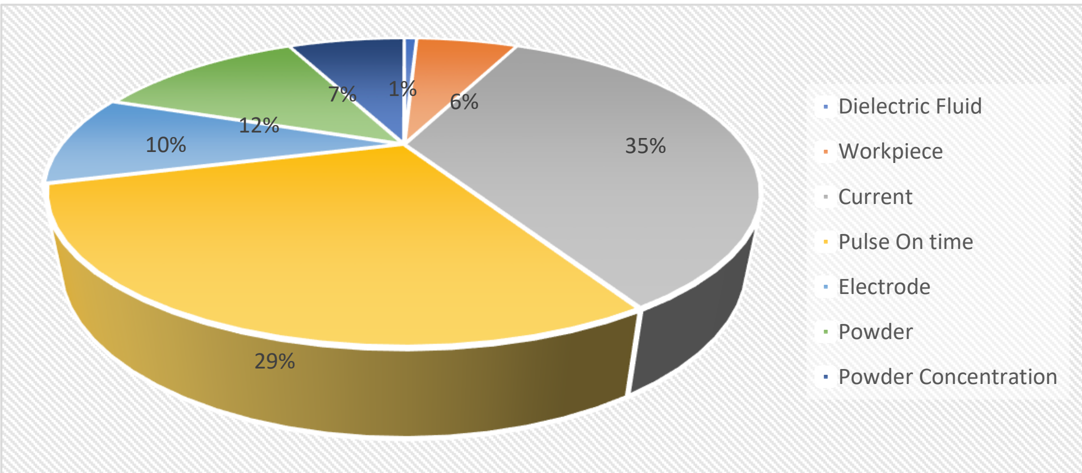

Figure 9. Percentage contribution of different control parameters persuading MRR

Table 11: Analysis of Variance for Mean of MRR

Source	DF	Seq SS	Adj SS	Adj MS	F	P
DF	1	1.233	1.233	1.233	0.37	0.573
Workpiece	2	24.728	24.728	12.364	3.76	0.121
Current	2	193.969	193.969	96.985	29.49	0.004
Pulse On Time	2	166.328	166.328	83.164	25.29	0.005
Electrode	2	56.103	56.103	28.051	8.53	0.036
Powder	2	74.964	74.964	37.482	11.40	0.022
Powder Concentration	2	69.662	69.662	34.831	10.59	0.025
Residual Error	4	13.156	13.156	3.289		
Total	17	600.143				

4.3 Investigation of tool wear ratio (TWR)

There is no dynamic contact between the electrodes during the EDM process; instead, the electrodes are eroded by the spark erosion phenomena [10]. Different tool materials used in PMEDM procedures exhibit varied degrees of tool wear because they have different densities, melting temperatures, electrical conductivity, and thermal conductivity.

Tool wear rate (TWR) is defined as the ratio of the eroded volume of tool material to the time required to machine the workpiece sample, typically expressed in mm^3/min. Experimental results indicate that the TWR for various steel alloys ranges from a minimum of 0.630 mm^3/min to a maximum of 1.755 mm^3/min. Figure 10 illustrated that the TWR significantly rises by increasing I_P and T_{ON}; whereas, increasing C_P decreases the TWR. This could be because of the enormous spark energy generated between the electrodes at high I_P and T_{ON}. Mixing conductive particles into dielectric media enhances breakdown across the spark gap (S_G) and increases the spark gap between electrodes. This reduces the insulating strength of the dielectric fluid (D_F) and facilitates easy short circuits. As a result, immediate explosions and rapid sparking occur during discharge, leading to accelerated erosion of the tool material. It can be also seen from Fig. 10 that Cu powder generates least amount of tool wear, followed by Cr powder and W powder. Besides, it can be seen that the type of D_F has no effect on TWR.

Furthermore, graphite tool removes the maximum tool material, preceded by Cu and W-Cu tool materials [15]. This could be validated in the same way that the influence of tool material on MRR could be. Besides, TWR is high during EN 31 machining, preceded by AISI 1040 and HCHCr steel. Figure 11 displays the S/N ratio plot for the influence of input parameters on TWR value.

The ANOVA approach's findings indicate that C_P, I_P, T_{ON}, and M_E have the greatest effects on TWR. However, it is discovered that DF has the least impact on TWR. The most important variables that affect TWR, according to Figure 12, are C_P (32%), I_P (25%), and T_{ON} (15%). According to Table 6, during machining HCHCr steel with a graphite tool at 7 An I_P and 180 µs T_{ON} while using tungsten powder mixed EDM oil, the minimal TWR of 0.630 mm^3/min is reached.

Further, ANOVA is performed to examine the significance of the control parameters on TWR. Table 12 shows the ANOVA table for mean of TWR. Table 12 reveals that the control parameters with p-value less than 0.05 significantly affect the multiple output characteristic i.e. TWR value. From Figure 12 and Table 12 it can be seen that powder concentration is the most significant factor influencing TWR.

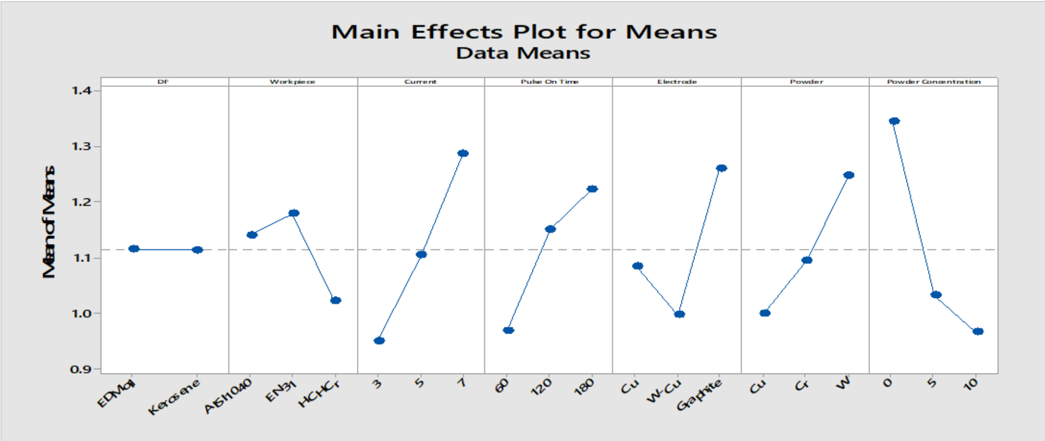

Figure 10. Main effect plot for control parameters (X-axis) on TWR (Y-axis)

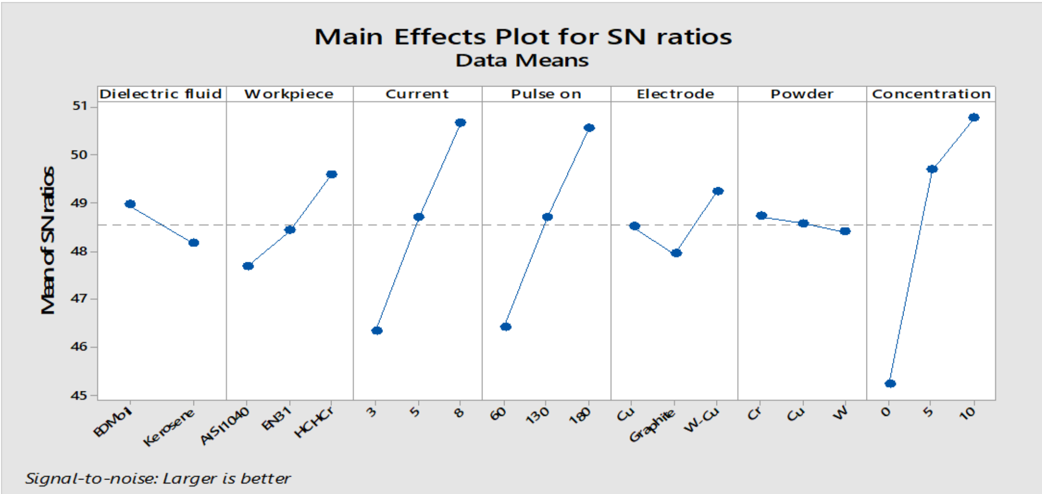

Figure 11. S/N ratio analysis for various control parameters on TWR

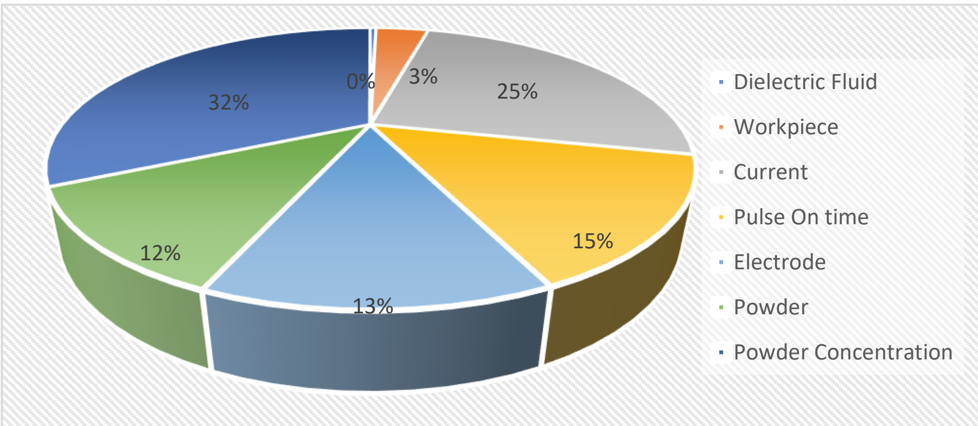

Figure 12. Proportion contribution of different control parameters effecting TWR

Table 12: Analysis of Variance for Mean of TWR

Source	DF	Seq SS	Adj SS	Adj MS	F	P
DF	1	0.00000	0.000000	0.000000	0.00	0.995
Workpiece	2	0.07983	0.079828	0.039914	5.33	0.075
Current	2	0.34007	0.340067	0.170033	22.69	0.007
Pulse On Time	2	0.20671	0.206708	0.103354	13.79	0.016
Electrode	2	0.21453	0.214533	0.107266	14.32	0.015
Powder	2	0.18853	0.188531	0.094265	12.58	0.019
Powder Concentration	2	0.48673	0.486726	0.243363	32.48	0.003
Residual Error	4	0.02997	0.029970	0.007492		
Total	17	1.54636				

4.4 Multi-response optimization

Furthermore, the multiple responses are optimised using the TOPSIS algorithm, which is based on fuzzy logic. As discussed in the previous section, the fuzzy TOPSIS method quantifies the closeness coefficient (CC_i) value for each trial of the L_{18} OA.

The findings of all CCi values from all 18 trials are shown in Table 13, which demonstrates that experiment No. 8 yields the greatest CCi value. Thus, among the 18 tests, experiment No. 8's control factor configuration ensures the best value of controls for the anticipated response variables. The control factors setup of experiment No. 8 thus offers the finest multiple performance characteristic among the aforementioned 18 experiments and is ranked first. Similar to this, the CCi values of all 18 studies were ranked in decreasing order. As per the ranking of all 18 experiments noted in Table 13, the optimum machining performances for the powder mixed EDM (Ra= 5.9830 µm, MRR= 27.2428 mm^3/min, and TWR= 0.7745 mm^3/min) were obtained for EDM oil (A1), AISI 1040 steel (B3), 5 An I_P (C2), 180 µs T_{ON} (D3), W-Cu tool (E2), copper powder (F1), and 10 g/lit powder concentration (G3). Lower values of Ra (surface roughness) and TWR (tool wear rate) are desirable, while a higher MRR (material removal rate) is also sought, creating a conflict among these response variables. To find the optimal values for these conflicting outputs, it's essential to consider the perspectives of multiple decision-makers regarding the importance of each response. According to Table 8, MRR is identified as the most critical response variable, followed by surface roughness and then TWR. However, from the above study it was witnessed that T_{ON}, I_P, and C_P were the most affecting factors to fulfil the desired output responses. Therefore, the optimum value of multiple responses was noted at high T_{ON}, moderate I_P, and high C_P. Furthermore, using copper powder mixed with EDM oil is most effective for optimizing multiple response variables. Copper powder offers moderate Ra and MRR while achieving the lowest TWR. Meanwhile, EDM oil results in lower Ra and higher MRR compared to kerosene dielectric fluid, although it has a negligible effect on TWR. This combination allows for a well-rounded performance in the machining process.

Table 13: Values of CC_i of 18 set of trials and their Ranks

S.NO:	DF	Workpiece	Current (A)	T_{ON} (µs)	Electrode	Powder	Concentration (g/l)	Closeness coefficient (CC_i)	Rank
1	EDM oil	HCHCr	3	60	Cu	Cu	0	0.5348	10
2	EDM oil	HCHCr	5	120	W-Cu	Cr	5	0.5657	8
3	EDM oil	HCHCr	7	180	Graphite	W	10	0.5221	11
4	EDM oil	EN31	3	60	W-Cu	Cr	10	0.6073	6
5	EDM oil	EN31	5	120	Graphite	W	0	0.3568	18
6	EDM oil	EN31	7	180	Cu	Cu	5	0.4897	12
7	EDM oil	AISI1040	3	120	Cu	W	5	0.6629	3
8	EDM oil	AISI1040	5	180	W-Cu	Cu	10	0.7301	1
9	EDM oil	AISI1040	7	60	Graphite	Cr	0	0.3672	16
10	Kerosene	HCHCr	3	180	Graphite	Cr	5	0.4782	13
11	Kerosene	HCHCr	5	60	Cu	W	10	0.7017	2
12	Kerosene	HCHCr	7	120	W-Cu	Cu	0	0.3936	15
13	Kerosene	EN31	3	120	Graphite	Cu	10	0.6103	5
14	Kerosene	EN31	5	180	Cu	Cr	0	0.3501	17
15	Kerosene	EN31	7	60	W-Cu	W	5	0.5727	9
16	Kerosene	AISI1040	3	180	W-Cu	W	0	0.4635	14
17	Kerosene	AISI1040	5	60	Graphite	Cu	5	0.6133	4
18	Kerosene	AISI1040	7	120	Cu	Cr	10	0.5612	7

4.5 Investigation of white layer and micro-cracks

White layer thickness, recast layer formation and size, fracture and crater dimensions, microhardness (MH), and Ra (surface roughness) are common metrics for assessing surface quality in EDM processes [31]. The surface morphology of the EDMed sample has been evaluated using scanning electron microscopy (SEM) scans from an FEI Nova Nano SEM 450. According to the SEM data, the mixture of powder and dielectric fluid (DF) significantly reduces Ra and results in the formation of a white layer along with small cracks on the EDMed surface [12]. Figure 13 (a) and (b) illustrates SEM micrographs of HCHCr steel machined surfaces during two randomly selected experiments i.e. experiment no. 2 and experiment no. 3 respectively. Both the experiment was selected randomly and deals with the machining of HCHCr steel using EDM oil at different levels of I_P, T_{ON}, and C_P. Fig. 13 (a) shows a thick and irregular white layer formation and uniformly distributed globules when compared with Figure 13 (b). This may be due to the low energy produced at low level of I_P and T_{ON} which causes for less Ra but leading to thick and irregular white layer on machined sample [32].

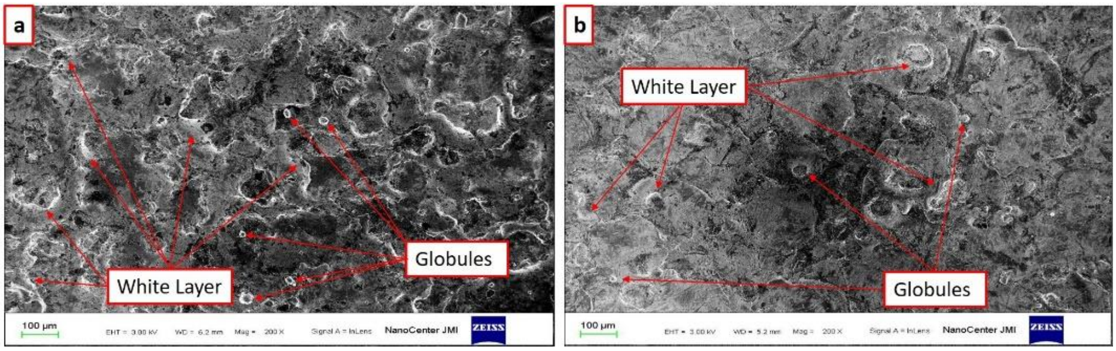

Figure 13. Illustrates the SEM images (100 µm) of HCHCr machined (a) using 5 g/L chromium powder mixed EDM oil and W-Cu electrode at 5 A I_P and 120 µs T_{ON} and (b) using 10 g/L tungsten powder mixed EDM oil and graphite electrode at 7 A I_P and 180 µs T_{ON}

It is evident from Figure 14 (a) and (b) that experiment number 2 results in the formation of thin, discontinuous fractures, whereas experiment number 3 results in thicker, continuous cracks. This might be a result of the experiment number three's high I_P (7 A) and high T_{ON} (180 µs). High discharge energy generated across the spark gap resulted in higher I_P and T_{ON}. The thicker and continuous fractures on the machined surface were formed as a result of the higher discharge energy's strong discharge impact force on the workpiece surface [11].

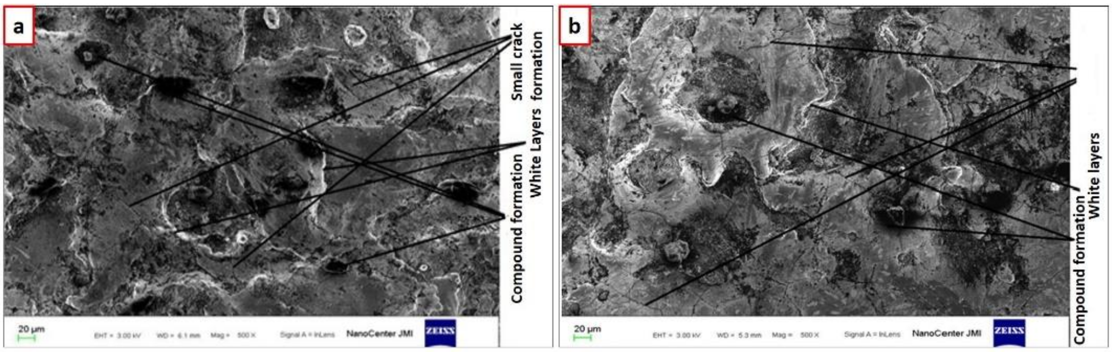

Figure 14. Illustrates the SEM images (20 µm) of HCHCr machined (a) using 5 g/L chromium powder mixed EDM oil and W-Cu electrode at 5 A I_P and 120 µs T_{ON} and (b) using 10 g/L tungsten powder mixed EDM oil and graphite electrode at 7 A I_P and 180 µs T_{ON}

From Figure 15 (a) a high recast layer can be observed as compared to the Figure 15 (b). This may be attributed to inadequate cooling of HCHCr steel when using chromium powder mixed with EDM oil. Since chromium powder has lower thermal conductivity compared to tungsten powder, it leads to slower cooling of the EDMed surface. This slower cooling process results in the formation of a thicker recast layer, as observed in the analysis. From Figure 15 (b) the enlargement of cracks can be observed as the concentration of powder increased which causes widening of the discharge column.

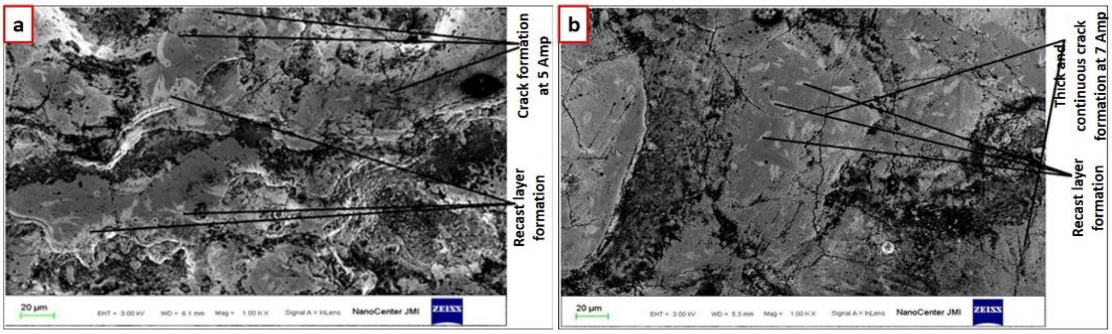

Figure 15. Illustrates the SEM images (20 µm) of HCHCr steel machined (a) using 5 g/L chromium powder mixed EDM oil and W-Cu electrode at 5 A I_P and 120 µs T_{ON} and (b) using 10 g/L tungsten powder mixed EDM oil and graphite electrode at 7 A I_P and 180 µs T_{ON}

The PMEDM process on the machined surface was analyzed using X-ray diffraction (XRD). The composite XRD pattern in Fig. 16 (a) reveals the presence of chromium powder in the EDM oil and W-Cu tool used for machining HCHCr steel, alongside copper and tungsten particles, as well as iron and chromium carbides (Fe_3C and Cr_3C_2). While tungsten powder may also have been present in the EDM oil and graphite tool, Fig. 16 (b) indicates the presence of iron carbide (Fe_3C), chromium carbide (Cr_3C_2), and particles of carbon and tungsten.

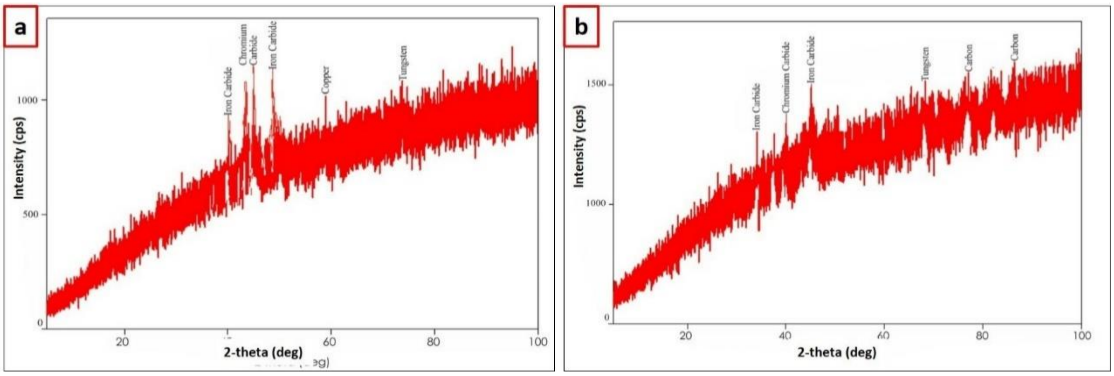

Figure 16. Illustrates XRD images of HCHCr steel machined (a) using 5 g/L chromium powder mixed EDM oil and W-Cu electrode at 5 An I_P and 120 µs T_{ON} and (b) using 10 g/L tungsten powder mixed EDM oil and graphite electrode at 7 A I_P and 180 µs T_{ON}

5. Conclusion

This paper presents a comprehensive study investigating the influence of different powder-mixed dielectrics, tool materials, and machining parameters during the EDM of various steel alloys. Additionally, a multi-criterion decision-making (MCDM) technique is employed to identify the optimal arrangement of process parameters for achieving the best performance characteristics. The findings offer valuable insights into the machining of different steel alloys using the PMEDM process.

The current work clarifies the multi-response optimization problem during the PMEDM of various steel alloys, including AISI 1040, EN 31, and HCHCr, using a fuzzy-based TOPSIS technique. Numerous experiments demonstrated the effects of electrical conductivity of the workpiece, tool, and powder, as well as the influence of pulse-on time (TON), input pulse (IP), and machinability during the PMEDM process. It was found that the Ra, MRR, and TWR were significantly affected by the physical characteristics of the powder particles and their concentration in the dielectric medium. Interestingly, the type of dielectric medium had the least impact on Ra, MRR, and

TWR. The results of the current experimental investigation are as follows:

i. The lowest Ra value of 2.2781 µm was achieved when machining HCHCr steel with a copper tool at 5 A IP and 60 µs TON, using a tungsten powder mixed with kerosene dielectric fluid.
ii. The maximum material removal rate (MRR) of 32.9992 mm³/min was obtained during the EDM of HCHCr steel using a tungsten powder mixed EDM fluid and a graphite tool at 7 An IP and 180 µs TON
iii. The lowest tool wear rate (TWR) was recorded when using a graphite tool for EDM on HCHCr steel at 7 An IP and 180 µs TON, with the lowest TWR value of 0.6295 mm³/min measured while using EDM oil combined with tungsten powder.
iv. The fuzzy TOPSIS results indicated that the control parameter setting of A1B3C2D3E2F1G3 from experiment number 8 yields the optimal values for multiple responses (Rank 1). In this experiment, the best recorded values were Ra = 5.9830 µm, MRR = 27.2428 mm³/min, and TWR = 0.6295 mm³/min.
v. It can be seen from the surface morphology that increasing the current from 5 A to 7 A and T_{ON} from 120 µs to 180 µs causes the surface of the EDMed sample to develop deep, and continuous fractures as well as thin white layers. The Ra of the EDMed sample has increased as a result of these large cracks.
vi. On the machined surface of HCHCr steel, SEM investigation revealed the presence of iron carbide (Fe_3C) and chromium carbide (Cr_3C_2) components together with some foreign elements including copper and tungsten.

6. Limitations and Future Scopes

Every benefit of any process, and indeed everything, comes with its own set of constraints. As a result, this process has some limitations as well, which are outlined below:

1. This study is focused on the influence of several input parameters on major EDM responses such as Ra, MRR, and TWR. However, effect of input parameters on micro-hardness can also be performed in future work.
2. In this study authors investigated the effect of different powder particles on EDM performance characteristics. However, the effect of particle size can be investigated in further study.
3. This work focused on the machining of various steel alloys i.e. conductive materials. However, machining of low conductive and insulating materials using EDM process can be performed in further study.
4. In this study the metallurgical characteristics of machined surface is not been considered. It can be the part of the further analysis of this work by performing microstructural and EDS analysis.
5. The membership function and defuzzification method can be considered for future research work.
6. Post-hoc tests (e.g., Tukey's HSD) can be performed to identify significant differences between factor levels.

References

[1] A. S. Walia, V. Srivastava, P. S. Rana, N. Somani, N. K. Gupta, G. Singh, D. Y. Pimenov, T. Mikolajczyk, and N. Khanna, "Prediction of tool shape in electrical discharge machining of EN31 steel using machine learning techniques," *Metals*, vol. 11, no. 11, p. 1668, 2021. DOI: 10.3390/met11111668.

[2] W. Konig and S. Rummenholler, "Technological and industrial safety aspects in milling FRP," *ASME Mach. Adv. Comp.*, vol. 45, no. 66, pp. 1–14, 1993. https://dokumen.pub/abrasive-water-jet-machining-of-engineering-materials-1st-ed-2020-978-3-030-36000-9-978-3-030-36001-6.html.

[3] W. F. Sales, J. Schoop, L. R. R. da Silva, A. R. Machado, and I. S. Jawahir, "A review of surface integrity in machining of hardened steels," *J. Manuf. Process.*, vol. 58, pp. 136–162, Oct. 2020. DOI: 10.1016/j.jmapro.2020.07.040.

[4] S. P. Sivapirakasam, J. Mathew, and M. Surianarayanan, "Multi-attribute decision making for green electrical discharge machining," *Expert Syst. Appl.*, vol. 38, no. 7, pp. 8370–8374, Jul. 2011. DOI: https://doi.org/10.1016/j.eswa.2011.01.026.

[5] K. Gupta, *Introduction to Abrasive Water Jet Machining*, 1st ed. Cham, Switzerland: Springer,

2020, pp. 1–11. DOI: 10.1007/978-3-030-36001-6_1

[6] R. Singh and J. S. Khamba, "Mathematical modeling of tool wear rate in ultrasonic machining of titanium," *Int. J. Adv. Manuf. Technol.*, vol. 43, no. 5, pp. 573–580, 2009. https://doi.org/10.1007/s00170-008-1729-5.

[7] G. Q. Wang, H. S. Li, N. S. Qu, and D. Zhu, "Investigation of the hole-formation process during double-sided through-mask electrochemical machining," *J. Mater. Process. Technol.*, vol. 234, pp. 95–101, 2016. https://doi.org/10.1016/j.jmatprotec.2016.01.010.

[8] A. K. Dubey and V. Yadava, "Laser beam machining—A review," *Int. J. Mach. Tools Manuf.*, vol. 48, no. 6, pp. 609–628, May 2008. DOI: https://doi.org/10.1016/J.IJMACHTOOLS.2007.10.017.

[9] M. Patel, S. Kumar, J. Jagadish, D. Y. Pimenov, and K. Giasin, "Experimental analysis and optimization of EDM parameters on HcHcr steel in context with different electrodes and dielectric fluids using hybrid Taguchi-based PCA-utility and CRITIC-utility approaches," *Metals*, vol. 11, no. 3, p. 419, Mar. 2021. https://doi.org/10.3390/met11030419.

[10] H. K. Kansal, S. Singh, and P. Kumar, "Effect of silicon powder mixed EDM on machining rate of AISI D2 die steel," *J. Manuf. Process.*, vol. 9, no. 1, pp. 13–22, Jan. 2007. 10.1016/S1526-6125(07)70104-4.

[11] M. N. Alam, A. N. Siddiquee, Z. A. Khan, and N. Z. Khan, "A comprehensive review on wire EDM performance evaluation," *J. Process Mech. Eng., SAGE Part E*, vol. 236, no. 4, pp. 1–23, Jan. 2022. DOI: https://doi.org/10.1177/09544089221074843.

[12] M. N. Alam, A. N. Siddiquee, and Z. A. Khan, "Machining of ZrO2 using wire EDM: An experiment based investigation via assisted electrode," *Adv. Mater. Process. Technol.*, vol. 9, pp. 1–18, Aug. 2023. https://doi.org/10.1080/2374068X.2023.2247284.

[13] J. P. Agrawal, N. Somani, and N. K. Gupta, "A systematic review on powder-mixed electrical discharge machining (PMEDM) technique for machining of difficult-to-machine materials," *Innovation Emerging Technol.*, vol. 11, pp. 1–11, Feb. 2024. https://doi.org/10.1142/S2737599424400024.

[14] P. S. Bains, S. S. Sidhu, H. S. Payal, and S. Kaur, "Magnetic field influence on surface modifications in powder mixed EDM," *Silicon*, vol. 11, no. 1, pp. 415–423, Feb. 2019. https://link.springer.com/article/10.1007/s12633-018-9907-z.

[15] A. S. Hameed, F. O. Hamdoom, and M. S. Jafar, "Influence of powder mixed EDM on the surface hardness of die steel," *ICSET 2019, IOP Publishing*, vol. 518, p. 032030, 2019. DOI: 10.1088/1757-899X/518/3/032030.

[16] F. Kazi, C. A. Waghmare, and M. S. Sohani, "Optimization and comparative analysis of silicon and chromium powder-mixed EDM process by TOPSIS technique," *Eng. Appl. Sci. Res.*, vol. 48, no. 2, pp. 190–199, Mar. 2021. Retrieved from https://ph01.tci-thaijo.org/index.php/easr/article/view/240334. https://www.thaiscience.info/Journals/Article/EASR/10994133.pdf

[17] M. Singh and S. Singh, "Comparative capabilities of conventional and ultrasonic-assisted electrical discharge machining of Nimonic Alloy 75," *J. Mater. Eng. Perform.*, vol. 31, pp. 1–13, 2022. https://doi.org/10.1007/s11665-022-06601-1.

[18] Y. Zhang, G. Zhang, Z. Zhang, Y. Zhang, and Y. Huang, "Effect of assisted transverse magnetic field on distortion behavior of thin-walled components in WEDM process," *Chin. J. Aeronaut.*, vol. 35, no. 2, pp. 291–307, Feb. 2022. https://doi.org/10.1016/j.cja.2020.10.034.

[19] B. Surekha, T. Sree Lakshmi, H. Jena, and P. Samal, "Response surface modelling and application of fuzzy grey relational analysis to optimise the multi response characteristics of EN-19 machined using powder mixed EDM," *Aust. J. Mech. Eng.*, pp. 1–11, Jan. 2019. https://doi.org/10.1080/14484846.2018.1564527.

[20] T. Roy and R. K. Dutta, "Integrated fuzzy AHP and fuzzy TOPSIS methods for multi-objective optimization of electro discharge machining process," *Soft Comput.*, vol. 23, no. 13, pp. 5053–5063, Jul. 2019. https://doi.org/10.1007/s00500-018-3173.

[21] P. R. Dewan and P. K. Kundu, "Optimization of parameters of powder added EDM of Nimonic C-263 using TOPSIS," *Sadhana*, vol. 49, no. 190, pp. 1–17, May 2024. DOI: 10.1007/s12046-024-02516-w.

[22] K. Paswan et al., "An analysis of microstructural morphology, surface topography, surface integrity, recast layer, and machining performance of grapheme nanosheets on Inconel 718 superalloy: Investigating the impact on EDM characteristics, surface characterizations, and optimization," *J. Mater. Res. Technol.*, vol. 27, pp. 7138–7158, Nov. 2023. DOI: https://doi.org/10.1016/j.jmrt.2023.11.080

[23] A. Kumar, S. Kumar, A. Mandal, and A. R. Dixit, "Investigation of powder mixed EDM process parameters for machining Inconel alloy using response surface methodology," *Mater. Today*

Proc., vol. 5, no. 2, pp. 6183–6188, Jan. 2018. DOI: 10.1016/j.matpr.2017.11.489. https://doi.org/10.1016/j.matpr.2017.12.225.

[24] N. HuuPhan, T. Muthuramalingam, N. N. Vu, and N. Q. Tuan, "Influence of micro size titanium powder-mixed dielectric medium on surface quality measures in EDM process," *Int. J. Adv. Manuf. Technol.*, vol. 109, pp. 797–807, 2020. DOI: https://doi.org/10.1007/s00170-020-05698-9.

[25] S. Ramesh and M. P. Jenarthanan, "Investigation of powder mixed EDM of nickel-based superalloy using cobalt, zinc and molybdenum powders," *Trans. Indian Inst. Met.*, vol. 74, no. 4, pp. 923–936, Apr. 2021. https://doi.org/10.1007/s12666-020-02170-w.

[26] H. Hong, A. T. Riga, J. M. Gahoon, and C. G. Scott, "Machinability of steels and titanium alloys under lubrication," *Wear*, vol. 162–164, pp. 34–39, Apr. 1993. http://dx.doi.org/10.1299/jsmec.46.107.

[27] H. Bisaria and P. Shandilya, "Experimental investigation on wire electric discharge machining (WEDM) of Nimonic C-263 superalloy," *Mater. Manuf. Process.*, vol. 34, no. 1, pp. 83–92, Jan. 2019. DOI: https://doi.org/10.1080/10426914.2018.1532589.

[28] P. V. Ramana, M. Kharub, J. Singh, and J. Singh, "On material removal and tool wear rate in powder contained electric discharge machining of die steels," *Mater. Today Proc.*, vol. 38, pp. 2411–2416, Jan. 2021. https://doi.org/10.1016/j.matpr.2020.07.382

[29] M. Shabgard and B. Khosrozadeh, "Investigation of carbon nanotube added dielectric on the surface characteristics and machining performance of Ti–6Al–4V alloy in EDM process," *J. Manuf. Process.*, vol. 25, pp. 212–219, Jan. 2017. https://doi.org/10.1016/j.jmapro.2016.11.016.

[30] M. Niamat, S. Sarfraz, H. Aziz, M. Jahanzaib, E. Shehab, and W. Ahmad, "Effect of different dielectrics on material removal rate, electrode wear rate and microstructures in EDM," *Procedia CIRP*, vol. 60, pp. 2–7, 2017. https://doi.org/10.1016/j.procir.2017.02.023

[31] D. R. Sahu and A. Mandal, "Critical analysis of surface integrity parameters and dimensional accuracy in powder-mixed EDM," *Mater. Manuf. Process.*, vol. 35, no. 4, pp. 430–441, Mar. 2020. https://doi.org/10.1080/10426914.2020.1718695.

[32] B. Gugulothu, V. Vidyapriya, P. Sharma, H. Venkatesan, and N. Pragadish, "Electric discharge machining: A promising choice for surface modification of metallic implants," *Mater. Manuf. Process.*, vol. 7, pp. 107–136, Aug. 2023. http://dx.doi.org/10.4018/978-1-6684-7412-9.ch007.